Zirconium mesostructures immobilized in calcium alginate for phosphate removal

Kyeong-Ho Yeon*, Heesu Park*, Seung-Hak Lee*, Yong-Min Park*, Sang-Hyup Lee*,†, and Masakazu Iwamoto**

*Center for Environmental Technology Research, Korea Institute of Science and Technology,
P.O.BOX 131, Cheongryang, Seoul 130-650, Korea
**Chemical Resources Laboratory, Tokyo Institute of Technology, Nagatsuta, Midori-ku, Yokohama 226-8503, Japan

Abstract−Eutrophication caused by the excessive supply of phosphate to water bodies has been considered as one of the most important environmental problems. In this study, the powder of zirconium mesostructure (ZM), which was prepared with the template of surfactant, was immobilized in calcium alginate for practical application and the resulting material was tested to evaluate the phosphate removal efficiency. Sorption isotherms and kinetic parameters were obtained by using the entrapped ZM beads with 30 to 60% of ZM. The maximum sorption capacity increased with the higher ZM content. Q_{max} in Langmuir isotherm was 51.74 mg/g for 60% of ZM with 7 mm of size. The smaller the particle size of the ZM beads, the faster the rate of phosphate removal, because the phosphate ions had less distance to reach the internal pores of the immobilized ZM beads. Chemical and electrochemical regeneration techniques were compared. Phosphates adsorbed on the ZM beads were effectively desorbed with NaCl, NaOH, and Na_2SO_4 solutions. An electrochemical regeneration system consisting of an anion exchange membrane between two platinum-coated titanium electrodes was successfully used to desorb and regenerate the phosphate-saturated ZM beads. Complete regeneration was reached under optimal experimental conditions. Chemical and electrochemical regeneration proved the reusability of the bead form of the entrapped ZM, and will enhance the economical performance of the phosphate treatment process.

Key words: Zirconium Mesostructure, Phosphate, Adsorption, Regeneration

INTRODUCTION

Phosphate, an essential nutrient for all organisms, has been extensively used in agriculture for profitable crop and livestock production as well as in many other industries. Its increased use generates large amounts of phosphate-containing wastes, which are usually discharged into receiving water bodies as a form of sewage effluents. This excessive supply of phosphate to lakes, rivers, and coasts causes eutrophication, which is considered as one of the most important environmental problems. To reduce eutrophication, stringent discharge limits of phosphates are being imposed by the environmental regulators in many countries. The limit of total phosphate in the effluent of wastewater treatment plants in South Korea is 2.0 mg/L.

Several chemical and biological methods can be used for the removal of phosphate [1-5]. Chemical dosing approach precipitates phosphates with lime, $Ca(OH)_2$, to form calcium hydroxyapatite, $Ca_5OH(PO_4)_3$, under alkaline conditions. A disadvantage of this method is the cost of the reagents. Furthermore, the reagents require safe handling and regular operator intervention, and also increased space for storage. Treatment using chemicals for phosphate removal also results in a higher sludge production, imposing associated sludge treatment and disposal problems. Biological methods are often based on the accumulation of intracellular polyphosphates by bacteria during alternating anaerobic and aerobic process cycles [6]. However, a disadvantage of this technology is that there must be anaerobic and aerobic stages for the treatment of the returned liquor.

A variety of adsorbents have been developed for phosphate removal: aluminum oxide [7,8], iron oxide [9-11], zirconium oxide [12], ion exchange resin [5], and basic yttrium carbonate [13]. In previous researches, most adsorbents made of metal oxide required acidic conditions for phosphate removal [7,12,14]. Recently, the mesoporous structures of zirconium sulfate synthesized by using a template of surfactants, have shown high sorption capacity for the phosphate without pH control [15-18]. And, several researchers have reported that the zirconium mesostructure (ZM) had high surface area and nano-sized regular pores in it, and showed 2-3 times higher phosphate sorption capacity than the commercial anion exchange resins [16]. Although the ZM presented highly effective sorption for single-existing phosphate in water, the powder form of ZM has been rarely applied due to the packing difficulty in a bed, decreasing free flow with the operation, high operating pressure caused by suspended solids accumulated in the bed. Moreover, the high cost of the powder severely limits its use for commercial purposes. A solution to these limitations is to immobilize the powder of ZM on a non-soluble support, thereby creating a bead or gel form. Immobilized ZM can be used repeatedly or continuously in different types of reactors and separated easily from soluble reaction products. This simplifies operations and ensures reusability of ZM.

Various immobilization techniques such as adsorption, covalent binding and entrapment have been introduced and widely used in catalysis [19]. The entrapment method was selected to immobilize the ZM because the ZM does not need to provide reactive sites. Entrapment can be defined as physical restriction of reaction materials within a confined space or a network. Gelation of polyanionic or polycationic polymers by the addition of multivalent counter ions is a simple method of entrapment. In this study, ZM was entrapped

---

†To whom correspondence should be addressed.
E-mail: yisanghyup@kist.re.kr

in calcium alginate (Ca-Alg) because of Alg's mild gelling properties and non-toxicity. The resulting material was tested to evaluate the removal efficiency for phosphate and characterize for its potential use in wastewater, especially reject water after sludge dewatering. In addition, several regeneration methods of the entrapped ZM saturated by phosphate ions were examined and the possibility of a continuous use of the materials was discussed.

MATERIALS AND METHODS

1. Synthesis of Zirconium Mesostructure

ZM was prepared from zirconium sulfate tetrahydrate $(Zr(SO_4)_2 \cdot 4H_2O$, Aldrich Chemical Co., USA) and cetyltrimethylammonium bromide $(CH_3(CH_2)_{15}N(CH_3)_3Br$, Aldrich Chemical Co., USA) by the procedure reported previously [15,20,21]. An aqueous solution of 2.5 g of CTAB, which was used as templates, was added to 85 g of deionized water. Inorganic solution was prepared by dissolving 4.55 g of $Zr(SO_4)_2 \cdot 4H_2O$ in 15 g of deionized water. Then two solutions were mixed, and vigorously stirred for 2 h. Upon mixing, white precipitates were observed in the solution. After stirring, the solution containing precipitates was statically heated at 100 °C for 48 h, and passed through 0.45 μm membrane filters to separate the solid phase. The filtered precipitates were rinsed with 5,000 ml of deionized water and dried at 80 °C for 12 h, and then ground to powder type for the experiments.

2. Entrapment of Zirconium Mesostructure in Calcium Alginate

Alginate is an anionic linear copolymer that consists of 1,4′-linked β-D-mannuronic acid and α-L-guluronic acid in different proportions and sequential arrangements [22]. To prepare the bead form of ZM entrapped in Ca-Alg, the powder of ZM (30 to 60%, w/v) was mixed with sodium alginate solution (10%, w/v) and then the mixture was stirred thoroughly to ensure complete mixing. 70% of ZM was also tested, but the resulting product turned out to be an unsuitable medium for experiments. This may be due to the low content of Ca-Alg, which provides the mechanical properties. As soon as the mixture was dripped into $CaCl_2$ (1%, w/v) and polyethylenimine (5%, w/v) solution by using a syringe, beads were formed. The bead size was changed by using syringes with different needle diameters (1-7 mm in diameter). After 3 h of hardening, the beads were separated from calcium chloride solution by vacuum filtration. They were rinsed on a filter for five times with deionized water and then transferred into a desiccator for the storage at room temperature.

The surface morphology of the entrapped ZM in Ca-Alg was observed with a field-emission scanning electron microscope (FE-SEM, S-4700, Hitachi, Japan). The ZM beads were fixed on a support with carbon tape and coated with platinum under argon atmosphere by using a platinum sputter module in a high-vacuum evaporator. The samples were then examined at 20 kV. All images were captured on black and white. An energy dispersive x-ray spectrometer (EDS) was also used in conjunction with SEM to confirm the chemical constituents of the surface. EDS spot analysis using a spot diameter of about 3 nm at selected areas on the samples was conducted.

To measure the hydraulic resistance of the medium in a column, the permeability of the entrapped ZM was calculated from the equation:

$$Permeability = \frac{J \times L}{\Delta P} \tag{1}$$

where J is the flux, L is the thickness of the medium, ΔP is the pressure difference across the medium.

3. Adsorption Characteristics of the Beads Entrapping ZM

To assess the affinity of phosphate ions into the beads, the distribution coefficient, K_d, was measured at various pH. First, the beads were washed with distilled water. The water remaining on the surface of the beads was wiped off. Fifty milliliters of 1,000 ppm phosphate solution and 50 cm^3 of sample beads were added to a test tube. The mixture was shaken for 24 h. K_d values were obtained from the equation, $K_d = M_{ZM}/M_S$, where M_{ZM} and M_S were the amounts of phosphate exchanged into one gram of ZM and 1 ml the solution, respectively.

Phosphate sorption capacity of the ZM entrapped in Ca-Alg was tested. Materials weighing between 0.20 g and 3.00 g were placed in 60 ml glass tubes with 50 ml of deionized water having phosphate concentration of 1,000 mg/L. The tubes were shaken on a rotary shaker (099ARD4512, Glas-Col Co., USA) for 24 h at room temperature (20 °C). Preliminary tests showed that shaking time of 12 h was sufficient for phosphate concentration to reach equilibrium. After shaking, solution was separated from solids by 0.45 μm membrane filters, and analyzed for the residual phosphate concentration by ion chromatography (DX-120, DIONEX, USA). Langmuir isotherm model was applied to evaluate the sorption capacity of the ZM beads. The Langmuir model can be described as below:

$$q_e = \frac{bQ_{max}C_e}{1 + bC_e} \tag{2}$$

where q_e represents for sorption amount at equilibrium, b for Langmuir constant, Q_{max} for maximum sorption amount of unit gram of material, C_e for the concentration in aqueous phase at equilibrium. Q_{max} and b are the Langmuir constants related to the adsorption capacity and energy of adsorption, respectively. The adsorption capacity is the number moles of solute adsorbed per unit weight of adsorbent in forming a complete monolayer on the surface. The adsorption energy is a constant representing the energy of interaction with the surface.

Adsorption kinetics of materials was evaluated with a series of 60 ml glass tubes containing 0.30-0.70 g of adsorbents and 50 ml of 1,000 ppm phosphate solution. The tubes were shaken on the rotary shaker, and each tube was taken at the predetermined time interval. Solution in the tubes was separated from solid phase by 0.45 μm membrane filters, and analyzed for the residual phosphate concentration. A pseudo-second order rate equation was used for describing the kinetics of sorption of phosphate ion [23]. The pseudo-second order model can be described as below:

$$\frac{dq_t}{dt} = k(q_e - q_t)^2 \tag{3}$$

where t represents for time, q_t (mg/g) for sorption amount at time t, q_e (mg/g) for phosphate sorption amount at equilibrium, k (g/mg·min) for pseudo-second order reaction rate constant.

4. Chemical and Electrochemical Regeneration of the ZM Beads

Adsorbent regeneration is an important operation which has a strong impact on the economical performance of adsorption pro-
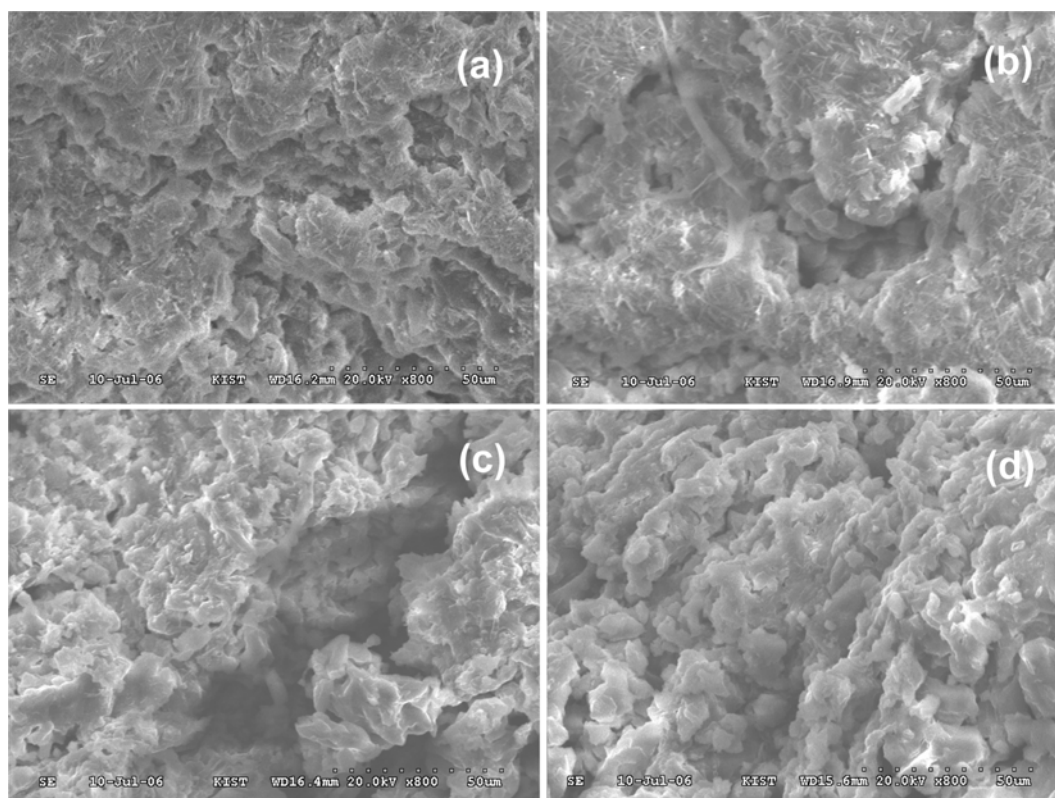
Fig. 1. SEM images of the entrapped zirconium mesostructures with different ZM content: (a) 30% of ZM, (b) 40% of ZM, (c) 50% of ZM, and (d) 60% of ZM in calcium-alginate.

cess. In this study, chemical and electrochemical regeneration methods of the exhausted ZM beads were evaluated. Chemical regeneration methods tested three different solutions: NaOH, NaCl, and Na_2SO_4 with 0.3 N to 1.0 N concentration. Electrochemical regeneration was achieved by using a dc voltage to create a current through the bed. The electrochemical cell consists of plate packing to fix the module, an anion exchange membrane (AMX, ASTOM, Japan) between two platinum-coated titanium electrodes, distributor for solution to flow, and gasket. The effective surface area was 50 cm^2, and 50 mL of ZM beads was packed in the device. Sodium hydroxide and phosphoric acid solution were circulated through the regeneration and recovery chamber, respectively. The effects of phosphoric acid concentration and current density on the recovery of phosphates were measured.

The efficiencies of the desorption of phosphates from the entrapped ZM and the regeneration of it using chemical and electrochemical methods were compared. For chemical regeneration, 3 g of the ZM beads saturated with phosphate (15.35 mg P/g) were added into 50 mL of each regenerating solution and shaken for 24 h at 25 °C. For electrochemical regeneration, 0.1 M sodium hydroxide and 0.01 M phosphoric acid were circulated and a current of 25 mA/cm^2 was applied. The ZM beads obtained by these procedures were put into the Langmuir isotherm tests and k and q_e values were calculated to compare with the initial values.

RESULTS AND DISCUSSION

1. Characteristics of the ZM Beads

The SEM/EDS investigation indicated the variation across the entrapped ZM surface and gave further insights into the nature of the material. SEM images showing the surface texture of the entrapped ZM with different ZM contents at 800-fold magnification are presented in Fig. 1. The images supported the ZM powders (white color) are immobilized by calcium alginate (dark gray color). The white portion increased with the content of ZM powders. The associated EDS analyses also confirmed that ZM was successfully entrapped in Ca-Alg by showing the relatively high levels of C, O, Zr, and S. Quite low levels of Al and Cl were also present (Fig. 2).

The permeability of a medium is a function of particle diameter, packing, size distribution, asymmetry, etc. The medium permeability has significant impacts on the design of a reactor as well as on the process economics [24,25]. The permeability tests were conducted by using a glass column with 30 mm of diameter and 150 mm of length, and the results are summarized in Table 1. Amberlite IRA 402 ion exchange resin, a widely used strong basic anion exchange resin in the environmental applications, was used for comparison with the ZM beads. The permeability of the ZM beads with 7.0 mm was higher than those of the others due to its larger size. The permeabilities decreased as bead diameters or porosities were reduced. And, the bead form of the entrapped ZM proved to be applicable in water treatment plants because their permeability values were similar to that of Amberlite resin.

2. Effects of the pH on the Removal of Phosphate

Fig. 3 shows the pH dependence of the K_d values of phosphate ion. The predominant ion species is $H_2PO_4^-$ at pH values between 2.1 and 7.2, while HPO_4^{2-} predominates at pH 7.2-12.3. The result

30 % ZM in Ca-Alg (Zr 66.67%)   40 % ZM in Ca-Alg (Zr 73.00%)

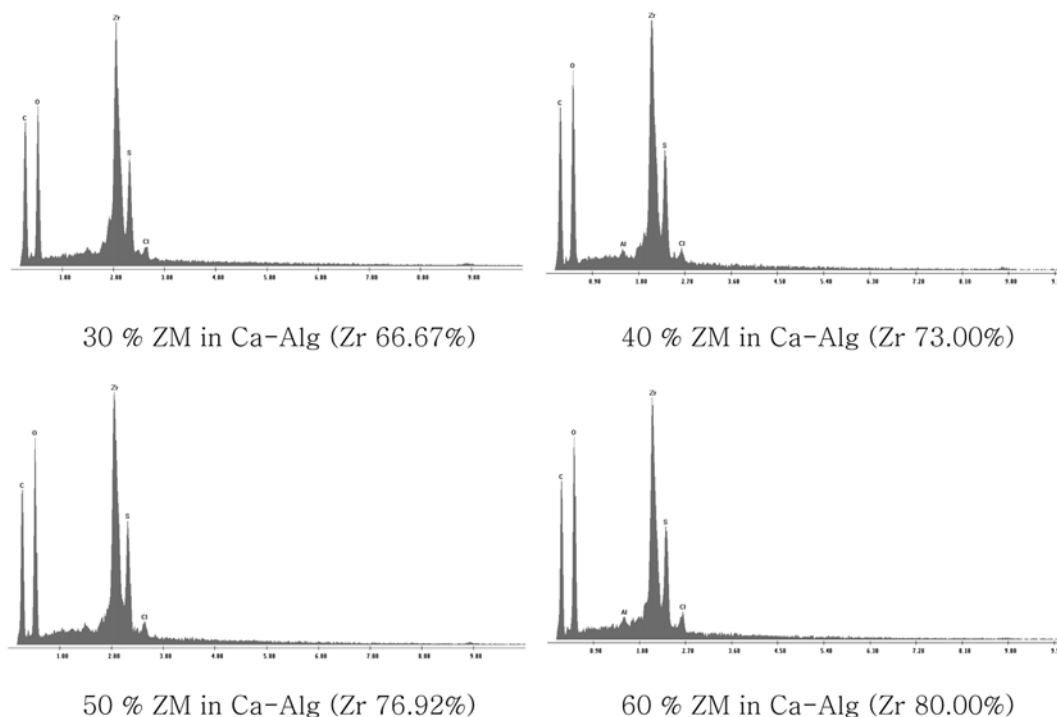50 % ZM in Ca-Alg (Zr 76.92%)   60 % ZM in Ca-Alg (Zr 80.00%)

Fig. 2. Analysis of zirconium peaks from energy dispersive x-ray spectrometer.

Table 1. Permeability of the resin and the entrapped zirconium mesostructures

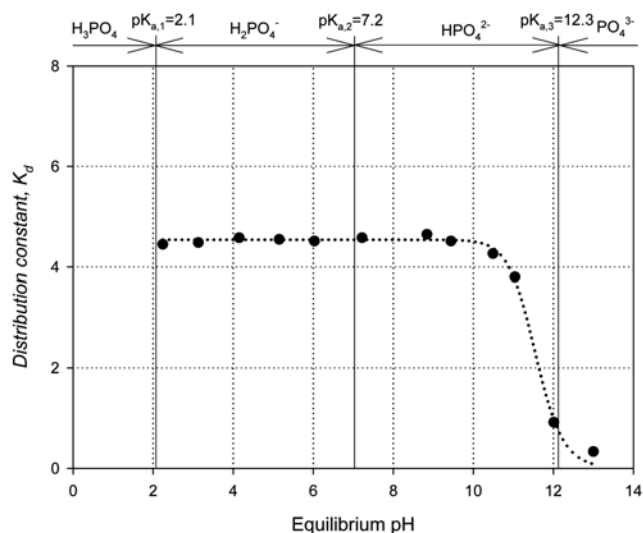| Media	Diameter (mm)	Permeability (l/m·hr·MPa)
Anion exchange resin (Amberlite IRA 402Cl)	0.7	49,930
ZM in calcium alginate	1.0	58,909
	3.0	79,880
	7.0	132,000

Fig. 3. Variation in K_d with pH of solution. Conditions: initial phosphate concentration=1,000 ppm; equilibrium time=24 h; ZM bead dosage=0.20 g; and at 20 ºC.
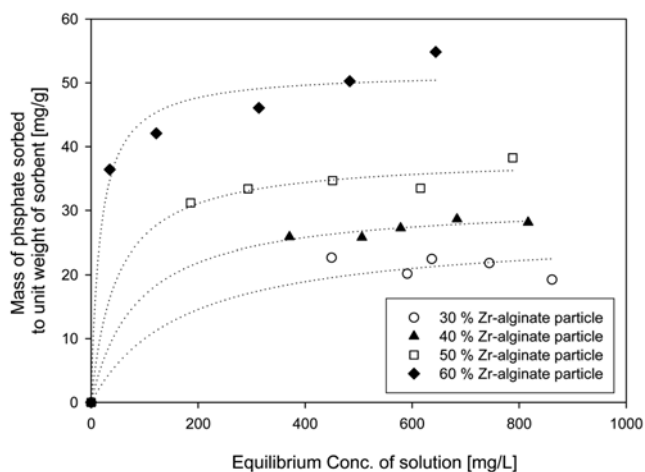

Fig. 4. Phosphate adsorption isotherms on the zirconium mesostructures synthesized with different ZM content in calcium alginate. Conditions: initial phosphate concentration=1,000 ppm; equilibrium time=24 h; dosage=0.30-1.0 g; and at 20 ºC.

indicated that the K_d for ZM was independent of equilibrium pH in the range of 2-11. The K_d values decreased significantly at pH 12 and higher. This reduction could be explained as that HSO_4^- ions in ZM were exchanged into 0.01 N (pH 12) of OH^- ions rather than 0.0035 N (1,000 ppm) of phosphate ions due to the concentration difference. Hence, for the following studies, the experiments were performed in a solution at pH values below 10.

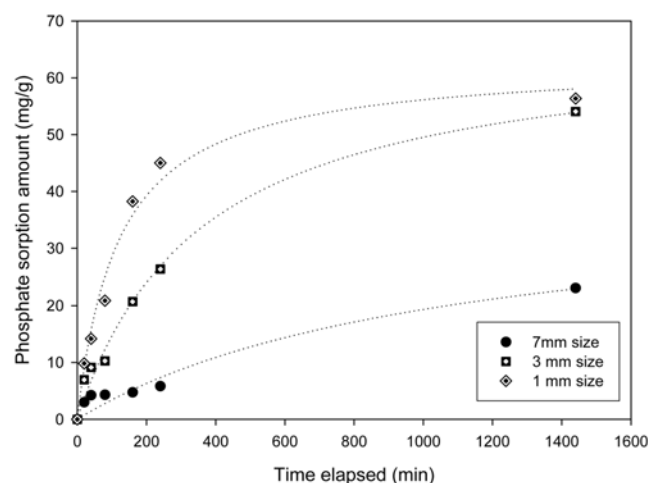**3. Phosphate Adsorption by the Entrapped ZM**

ZM powder in the beads offers the sorption capacity. Therefore, the properties of the entrapped ZM were greatly influenced by the

Table 2. Langmuir parameters of the entrapped zirconium meso-structures with different ZM content in calcium alginate (size: 7 mm)

Percent of zirconium mesostructures	Q_{max} [mg/g]	b [L/kg]	r^2
30%	26.95	0.006	0.98
40%	31.31	0.012	0.99
50%	38.44	0.021	0.99
60%	51.74	0.058	0.98

Table 3. Kinetic parameters of zirconium mesostructures synthesized with different ZM content in calcium alginate (size: 7 mm)

Percent of zirconium mesostructures	k [g/mg min]	q_e [mg/g]	r^2
30%	1.17×10^{-4}	23.81	0.98
40%	0.65×10^{-4}	28.18	0.96
50%	0.30×10^{-4}	35.29	0.98
60%	0.23×10^{-4}	39.84	0.97

Table 4. Langmuir parameters of 60% zirconium mesostructures with different size

Diameter	Q_{max} [mg/g]	b [L/kg]	r^2
1 mm	67.99	0.050	0.97
3 mm	56.50	0.054	0.97
7 mm	51.74	0.058	0.98

Table 5. Kinetic parameters of 60% zirconium mesostructures synthesized with different size

Size	k [g/mg min]	q_e [mg/g]	r^2
1 mm	1.00×10^{-4}	62.89	0.99
3 mm	0.41×10^{-4}	59.33	0.99
7 mm	0.23×10^{-4}	40.08	0.99

Fig. 5. Phosphate adsorption kinetics of the entrapped zirconium mesostructures with different diameter. Conditions: initial phosphate concentration=1,000 ppm; equilibrium time=24 h; ZM content=60% w/v; dosage=0.30-1.0 g; bead size (mean diameter)=1±0.17, 3±0.15, 7±0.12 mm; and at 20 ℃.

Fig. 6. Schematic diagram of the electrochemical regeneration system for the bead type of the entrapped zirconium mesostructures.

ratio of ZM powder to Ca-Alg. Fig. 4 shows the phosphate adsorption isotherms on the ZM beads synthesized at ZM content from 30% to 60% in calcium alginate. Q_{max} and b were determined from the Langmuir plots and the values are summarized in Table 2. It is evident that the maximum sorption capacity (Q_{max}) of the ZM beads increases with the ZM content. The Q_{max} for the beads with 60% of ZM was 51.74 mg/g or 1.63 meq/g.
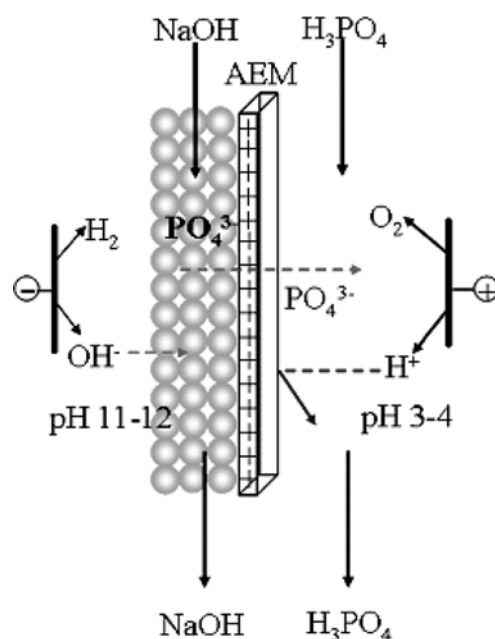
Table 3 presents the results of phosphate sorption kinetics and pseudo-second order model fitting on the zirconium mesostructures synthesized at different ZM contents in Ca-Alg. The reaction rate constants (k), corresponding to the removal rate of phosphate from the solution, decreased with increasing the ZM content. When high content of ZM exists, more external surface is covered by ZM. This can reduce or block the opening of the capillary pores that offer the paths of phosphate ions to the sorption sites within the Ca-Alg.

To investigate the effect of particle size on performance, the isotherms and kinetic tests on the entrapped ZM of diameter ranging from 1 to 7 mm were conducted. The smaller the particle size of the beads, the faster the rate of removal, because the phosphate ions have less distance to go to reach the pores within the beads (Fig. 5, Tables 4 and 5). The pseudo second-order kinetic constant k of the ZM beads with 1 mm size was 1.00×10^{-4} g/mg min, and the k value was reduced to 0.23×10^{-4} g/mg min when the bead size increased to 7 mm.

4. Regeneration of the Entrapped ZM

Fig. 6 is a schematic diagram of ion transport during the electrochemical regeneration process. Phosphate ions adsorbed on the ZM

beads are replaced with hydroxide ions generated at a cathode. The desorbed phosphate ions penetrate through the AEM and move to the next chamber where the phosphate ions meet the hydrogen ions generated at an anode and they form H_3PO_4. After the regeneration, the entrapped ZM materials take their hydroxide form.

The advantage of electrochemical regeneration is no need for desorption and/or regeneration solution. Hydroxide ions and hydrogen ions generated by electrical field are consumed during the regeneration process. Therefore, storage space for chemicals is not needed. In addition, the system can be operated continuously. The ZM beads are stored into the device and the influent containing phosphates is run through the system and ZM beads remove the phosphates from the solution. After the beads are saturated with phosphates and the removal efficiency get decreased, electrical current is provided by using a dc voltage to regenerate the ZM beads.

The effect of the concentration of the circulating phosphoric acid was tested between 0.01 M to 0.50 M at 0.1 M of NaOH and current density of 25 mA/cm^2. Table 6 indicates that the phosphates

Table 6. Variation of phosphate recovery with the concentration of phosphoric acid in an electrochemical module

Phosphoric acid (M)	Recovery (%)
0.01	95
0.05	88
0.10	71
0.50	57

Table 7. Variation of concentration of phosphoric acid on the current density in an electrochemical module

Current density (mA/cm^2)	Phosphoric acid (M)
25	1.74
30	2.01
40	2.74
50	3.12

Table 8. Chemical and electrochemical regeneration of the bead form of the entrapped zirconium mesostructures

Regeneration solution			k [g/mg min]	q$_e$ [mg/g]	r^2
Chemical regeneration	NaOH	0.3 N	435×10^{-4}	46.38	0.99
		0.5 N	312×10^{-4}	46.71	0.99
		0.7 N	298×10^{-4}	46.94	0.99
		1.0 N	384×10^{-4}	46.71	0.99
	NaCl	0.3 N	255×10^{-4}	47.07	0.99
		0.5 N	148×10^{-4}	48.17	0.99
		0.7 N	112×10^{-4}	49.43	0.99
		1.0 N	106×10^{-4}	49.56	0.99
	Na$_2$SO$_4$	0.3 N	193×10^{-4}	47.35	0.99
		0.5 N	181×10^{-4}	47.57	0.99
		0.7 N	182×10^{-4}	47.46	0.99
		1.0 N	175×10^{-4}	47.74	0.99
Electrochemical regeneration			231×10^{-4}	47.86	0.99
Initial ZM beads (7mm)			194×10^{-4}	47.55	0.99

were desorbed more with a lowering phosphoric acid concentration. The best recovery was obtained at 0.01 M of phosphoric acid. High level of circulating phosphoric acid could interfere with the transport of phosphate ions to the anode by concentration gradient. But, it should be noticed that a concentration lower than 0.01 M increased the electrical resistance and consumed more electricity.

Table 7 shows that the concentration of phosphoric acid was proportional to the current density applied to the cell. The concentration of circulating phosphoric acid reached 1.74 M at the current density of 25 mA/cm^2, and it doubled when 50 mA/cm^2 was provided. But, operational costs need to be considered because the electricity consumption increased by 4.0, 8.2, 11.7, and 18.7 kwh/ton.

The performance of several regeneration methods can be compared by using k and q$_e$ values from Eq. (3). The results are presented in Table 8. Three chemical solutions effectively desorbed the phosphates from the ZM_Ca-Alg. However, the lower q$_e$ values suggest that chemical regeneration with sodium hydroxide failed to provide complete restoration of the initial adsorption capacity. Sodium chloride and sodium sulfate solutions with concentration of 0.5 N and higher restored the adsorption capacity completely in terms of q$_e$. However, k values were not fully recovered. An electro-regeneration system was successfully used to desorb and regenerate the phosphate-saturated ZM beads. Complete regeneration was reached under optimal experimental conditions. Phosphate resources will be exhausted within several decades. Therefore, a phosphate recovery process should be incorporated with a phosphate removal system [26]. The enriched phosphates in the circulating solution could be recovered as a precipitate of calcium phosphate by addition of CaCl$_2$. The returned calcium phosphates can be recycled as a fertilizer.

CONCLUSIONS

ZM was prepared by using a surfactant as a template and it was successfully entrapped in calcium alginate for practical application. The phosphate sorption by the entrapped ZM was investigated by Langmuir isotherm and kinetic tests. The phosphate sorption by the ZM beads was not affected by pH variation from 2 to 11. The maximum sorption capacity increased with the higher ZM content. The smaller the particle size of the ZM beads, the better the access to the pores within the beads and the faster the rate of adsorption kinetics. The 1 mm of bead containing 60% of ZM showed the best performance for phosphate sorption with Q$_{max}$ of 67.99 mg/g. Phosphates adsorbed on the ZM beads were effectively desorbed with NaCl, NaOH, and Na$_2$SO$_4$ solutions. Complete regeneration of the exhausted ZM beads was reached under optimal experimental conditions with an electro-regeneration system. Chemical and electrochemical regeneration proved the reusability of the bead form of the entrapped ZM, and suggested the enhanced economical performance of the phosphate treatment process.

REFERENCES

1. M. I. Aguilar, J. Saez, M. Llorens, A. Soler and J. F. Ortuno, *Water Res.*, **36**, 2910 (2002).
2. D. Brdjanovic, A. Slamet, M. C. M. van Loosdrecht, C. M. Hooijmans, G. J. Alaerts and J. J. Heijnen, *Water Res.*, **32**, 200 (1998).
3. J. M. Ebeling, P. L. Sibrell, S. R. Ogden and S. T. Summerfelt, *Aquacult Eng.*, **29**, 23 (2003).
4. Y. Jaffer, T. A. Clark, P. Pearce and S. A. Parsons, *Water Res.*, **36**, 1834 (2002).
5. X. P. Zhu and A. Jyo, *Water Res.*, **39**, 2301 (2005).
6. M. T. L. Meganck and G. M. Faup, Eds., *Enhanced biological phosphorus removal from watewaters*, CRC Press, Roca Raton, FL (1988).
7. K. Urano and H. Tachikawa, *Ind. Eng. Chem. Res.*, **30**, 1893 (1991).
8. T. Hano, H. Takanashi, M. Hirata, K. Urano and S. Eto, *Water Sci. Technol.*, **35**, 39 (1997).
9. L. Zeng, X. M. Li and J. D. Liu, *Water Res.*, **38**, 1318 (2004).
10. O. Bastin, F. Janssens, J. Dufey and A. Peeters, *Ecol. Eng.*, **12**, 339 (1999).
11. R. A. Berner, *Earth. Planet. Sc. Lett.*, **18**, 77 (1973).
12. E. Kobayashi, K. Uematsu, Y. Nagawa and M. Sugai, *Nippon Kagaku Kaishi*, 1412 (1982).
13. M. J. Haron, S. A. Wasay and S. Tokunaga, *Water Environ. Res.*, **69**, 1047 (1997).
14. D. Y. Zhao and A. K. Sengupta, *Water Sci. Technol.*, **33**, 139 (1996).
15. H. Takada, Y. Watanabe and M. Iwamoto, *Chem. Lett.*, **33**, 62 (2004).
16. M. Iwamoto, H. Kitagawa and Y. Watanabe, *Chem. Lett.*, 814 (2002).
17. S. H. Lee, B. C. Lee, K. W. Lee, Y. S. Choi, K. Y. Park and M. Iwamoto, in *Wastewater reclamation & reuse for sustainability*, IWA specialty conference, Jeju, South Korea (2005).
18. P. Wu and M. Iwamoto, *Chem. Lett.*, 1213 (1998).
19. P. McMorn and G. J. Hutchings, *Chem. Soc. Rev.*, **33**, 108 (2004).
20. U. Ciesla, S. Schacht, G. D. Stucky, K. K. Unger and F. Schuth, *Angew. Chem. Int. Edit.*, **35**, 541 (1996).
21. J. S. Reddy and A. Sayari, *Catal. Lett.*, **38**, 219 (1996).
22. H. Ertesvag and S. Valla, *Polym. Degrad. Stabil.*, **59**, 85 (1998).
23. Y. S. Ho and G. McKay, *Water Res.*, **34**, 735 (2000).
24. M. Mulder, *Basic principles of membrane technology*, Kluwer Academic Publishers, Netherlands (1996).
25. W. S. Winston Ho and K. K. Sirkar, in *Membrane handbook*, V. Goel, M. A. Accomazzo, A. J. DiLeo, P. Meier, A. Pitt, M. Pluskal and R. Kaiser Eds., Van Nostrand Reinhold, New York (1992).
26. K. Kuzawa, Y. J. Jung, Y. Kiso, T. Yamada, M. Nagai and T. G. Lee, *Chemosphere*, **62**, 45 (2006).